Desalination and Water Treatment
www.deswater.com

doi: 10.5004/dwt.2017.20209

63 (2017) 158–166
February

Removal of Pb^{2+} and Cd^{2+} from aqueous solution using thiol-functionalized multi-walled carbon nanotubes as adsorbents

Qiong Li, Fang Zhou, Jingang Yu, Xinyu Jiang*

School of Chemistry and Chemical Engineering, Central South University, Changsha 410083, China,
emails: 707057173@qq.com (Q. Li), 346817616@qq.com (F. Zhou), yujg@csu.edu.cn (J. Yu), jiangxinyu@csu.edu.cn (X. Jiang)

Received 8 March 2016; Accepted 30 August 2016

ABSTRACT

Multi-walled carbon nanotubes modified with thiol groups (denoted as MWCNTs–SH) was prepared using thiourea as sources for thiol groups in hydrobromic acid, which avoided complex steps via conventional synthetic methods. The characteristic results of elemental analysis (EA), scanning electron microscopy (SEM), X-ray photoelectron spectroscopy (XPS), and thermogravimetric analysis (TGA) showed that the thiol groups were grafted onto the MWCNTs successfully and the percent was very high, which was advantageous to the adsorption of metal ions. The effects of contact time, initial adsorbent content, solution pH and temperature on the adsorption of Cd(II) and Pb(II) with MWCNTs–SH were studied systematically. The pseudo-second-order kinetic equation fitted better than that of pseudo-first-order kinetic equation to describe the adsorption kinetics of the thiol-functionalized carbon nanotubes. The adsorption isotherms of Cd(II) and Pb(II) by MWCNTs–SH matched well with the Langmuir isotherm model with the maximum adsorption capacities of 157.73 and 187.27 mg/g, respectively. The values of ΔG^{θ} and ΔH^{θ} calculated from the experiment data indicated that the adsorption process was spontaneous and endothermic in nature.

Keywords: Heavy metal adsorption; Thiol functional groups; Multi-walled carbon nanotubes; Kinetics

1. Introduction

Environmental pollution with heavy ions mainly comes from many industries, such as mining, metal processing, rubber, leather, plastic and medicine. Nowadays, the treatment and disposal of wastewater containing heavy metal ions is one of the most serious environment problems in the modern life [1]. Heavy metal ions are known pollutants that not only affect the ecological systems but also cause irreversible damage to human health, and the toxicity is not easy to eliminate [2]. The most common poisonous heavy metal ions, including lead, mercury, zinc, nickel and copper, are different from other pollutants due to their accumulation in living organisms [3,4]. The effluents of mining and related industries have to be treated carefully before discharge because the regulations worldwide have grown stricter [5]. Therefore, developing environmentally friendly technologies to decontaminate water efficiently is important for environmental monitoring and human health. Various separation methods including chemical precipitation [6], ion exchange [7], membrane filtration [8], flotation and adsorption [9] have been developed to remove heavy metal ions from aqueous solutions. Among the different treatments described above, the adsorption technology with no chemical degradation is recognized as one of the most effective methods for removing heavy metal ions due to the merits of efficiency, simplicity and economy. Numerous adsorbents, primarily including activated carbons, zeolites, industrial by-products, agricultural wastes, biomass and polymeric materials, have been developed to remove heavy metal ions from wastewater [10,11]. However, efforts are still needed to investigate for new promising adsorbents because of the low adsorption capacities of these adsorbents described above.

* Corresponding author.

Recently, carbon nanotubes (CNTs) have been investigated extensively and multi-disciplinarily due to their unique electrical, optical, mechanical and chemical properties [12]. Because of these excellent properties, CNTs perform great promise for potential applications in many technological fields such as catalyst supports, nanoelectronic devices, hydrogen storage and chemical senor [13]. It has also been proved that CNTs can be used to remove various pollutants such as dyes, phenols, aniline and divalent metal ions from aqueous solutions due to the π–π interactions, electrostatic interactions and large specific surface areas [14]. Although CNTs possess various excellent properties, the problems of insolubility limit their application because of the strong intermolecular van der Waals interactions between tubes [15]. A common and effective approach to improve dispersion and enhance the adsorption capability of CNTs is through chemical functionalization, which is used relatively often to generate functional groups on the surface of CNTs. In recent studies, oxidation of CNTs with functional groups (e.g., COOH, OH, C=O, OSO_3H) have been found to be good adsorbents for the removing of heavy metal ions, organic dyes, and oil [16]. Many other functional groups could also be appropriate for metal ion adsorption. For example, functionalized CNTs containing amion functional groups have attracted much attention because of their unique properties derived from the presence of amino groups and have been used to remove heavy metal ions from water [17,18]. A good candidate for heavy metal ions adsorption using surface modification of CNTs is the sulfur-containing functionality [19,20]. In particular, sulfur-containing groups have shown a strong propensity to interact with heavy metal ions [21–23]. In our previous work, CNTs containing dithiocarbamate groups were prepared and used to remove Cd(II), Cu(II) and Zn(II) from aqueous solution with high performance [24]. Therefore, efficient adsorbents made by introducing thiol groups onto MWNTs are very worth to expect.

According to the principle of hard and soft acids and bases (HSAB), thiol groups are named soft bases, and therefore it is reasonable to use thiol groups' functional materials to remove soft acids like Hg(II), Pb(II) and Cd(II), etc. [21,23]. But regarding the approaches to introduce thiol groups onto the surfaces of CNTs, a number of the conventional methods have been reported [21]. However, the experiment processes always involve more than two steps. In this paper, the thiol-functionalized material was realized according to the previous study [25], in which oxidized MWCNT (MWCNTs–OH) were functionalized by thiourea without using complex intermediate steps. The morphology of MWCNTs–SH was characterized by elemental analysis (EA), scanning electron microscopy (SEM), X-ray photoelectron spectroscopy (XPS), and thermogravimetric analysis (TGA). The application of MWCNTs–SH for the removal of Cd(II) and Pb(II) from aqueous solution was investigated by the batch experiments.

2. Experimental

2.1. Materials

CNTs (purity > 95%) were purchased from Shenzhen Nanotech Port Co., Ltd. The range of diameters is 20–40 nm and the length exceeds 5 μm. The thiourea and hydrobromic acid were purchased from Sinopharm Chemical Reagent Co., Ltd. Metal salts including $Cd(NO_3)_2{\cdot}4H_2O$ and $Pb(NO_3)_2$ were used as sources for Cd(II) and Pb(II), respectively. All the chemicals used were of analytical grade and used as received without any further purification. Deionized water was prepared with a Milli-Q water purification system (Millipore, Milford, MA).

2.2. Synthesis of thiol-derivatized MWCNTs (MWCNTs–SH)

The synthesis procedure of MWCNTs–OH is as follows: 500 mg of raw multi-walled carbon nanotubes (r-MWCNTs) was dispersed in 30 mL $FeCl_2$ solution under mechanical stirring. 100 mL H_2O_2 was added slowly into the mixture, and then reacted for 12 h at room temperature with constant stirring [26]. Then the reaction solution was added to 10% HCl solution (100 mL) and the products were separated using a 0.45 μm PTFE membrane. The obtained products were washed with deionized water for several times and dried in a vacuum oven.

400 mg of MWCNTs–OH in 35 mL hydrobromic acid and 65 mL glacial acetic was reacted with 200 mmol thiourea under magnetic stirring at 110 °C for 48 h. Then, the hot mixture was poured into a cold (ice bath) 15% NaOH solution (600 mL), and stirred overnight at room temperature [25]. The reaction mixture was acidified with 50% aqueous HCl to pH 2–3, maintaining a temperature less than 10°C. The mixture was separated through a 0.45 μm PTFE membrane. The solid residuals were washed several times with deionized water. Finally, the obtained MWCNTs–SH was kept in a vacuum oven at 60°C for 24 h. The procedure for the functionalization of MWCNTs was depicted in Fig. 1.

2.3. Characterizations

TGA was performed using a NETZSCH STA 449C analyzer. The MWCNTs samples were heated at a rate of 10°C/min from room temperature to 700°C in a nitrogen atmosphere with a flow rate of 50 mL/min. XPS spectra were obtained using an ESCALab220i-XL electron spectrometer from VG Scientific, using Al K_α as the X-ray source. The microstructures of the MWCNTs samples were observed on a TESCAN MIRA3 LMH/LMU field emission scanning electron micro-scopes.

2.4. Adsorption experiments

All the batch adsorption experiments were conducted in 50 mL conical flasks containing 20 mL of Cd(II) or 30 mL of Pb(II) ion solution at setting conditions. The effects of

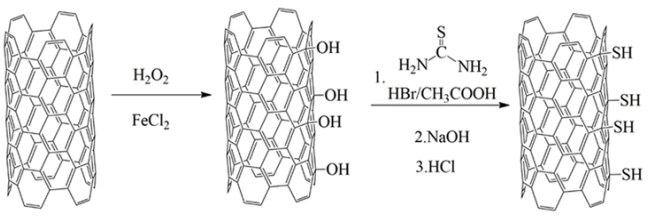

Fig. 1. Schematic illustration of synthetic route of MWCNTs–SH.

different solution pH values of the initial solution on adsorption were investigated in pH range of 2.0 to 6.0 to avoid the precipitation of metal hydroxides. The solution pH was adjusted by 0.1 mol/L HNO_3 and 0.1 mol/L NaOH solution. The flasks were agitated in a thermostatic water-bath shaker operated at 220 rpm for a certain time. Then, the adsorbents were filtered by a 0.45-μm pore size filter paper after the solution reached equilibrium. The residual concentration of each metal ion was measured by atomic absorption spectrophotometric method. The adsorption capacity of the adsorbent at equilibrium was calculated by the following equation:

$$q_e = \frac{C_o - C_e}{m} \times V \quad (1)$$

where q_e is the equilibrium adsorption capacity of metal ions (mg/g), C_o and C_e (mg/L) are the initial and equilibrium concentrations of metal ions, respectively, V is the volume of the solution (L), and m is the weight of the absorbent(mg).

In the kinetic experiments, the equilibrium contact time is necessary to determine at the beginning of the adsorption. The experimental procedure was performed as follows: 5.0 mg of adsorbent was weighed into the flasks with 20 mL of Cd(II) solution at a concentration of 10 mg/L or 30 mL Pb(II) solution at a concentration of 40 mg/L with pH 6.0 and 5.0, respectively. Then, the mixture was shaken at 220 rpm agitation speed in a shaking thermostatic bath at constant temperature for a contact time varied in the range of 0–120 min. The concentration of each metal ion solution was measured as mentioned previously. Each data point was obtained from an individual flask.

For the equilibrium adsorption experiments, the various initial concentrations of metal ions solution were changed from 10 to 60 mg/L in conditions of fixed amount of absorbent 5 mg per 20 mL and 30 mL ion solution for Cd(II) and Pb(II), respectively, constant pH 6.0 for Cd(II) and 5.0 for Pb(II) and 220 rmp agitation speed. The temperatures were maintained at 25°C, 35°C and 45°C.

All the duplicate experiments were carried out with fairly good reproducibility.

3. Results and discussions

3.1. Characterization of MWCNTs

The TGA was performed to evaluate the thermal stability of the functionalized MWCNTs. Fig. 2 shows the TGA curves of MWCNTs–OH and MWCNTs–SH. As shown in Fig. 2, the first weight loss below 180°C of MWCNTs–OH and MWCNTs–SH was confidently due to the loss of water which is present in external surface and internal pores or cavities [27]. The weight loss above 180°C of the MWCNTs–OH and MWCNTs–SH can be attributed to the thermal decomposition of the surface –OH and –SH groups. And the greater weight loss of MWCNTs–SH indicates the presence of thiol functional groups on the surface of MWCNTs. Therefore, according to the TGA data, the amount of thiol groups covalently bonded to the MWCNTs was estimated, based on the total weight of MWCNTs–OH, to be about 19.74 wt% in relation to the MWCNTs–SH. Element analysis confirmed the S content of the MWCNTs–SH (Table 1).

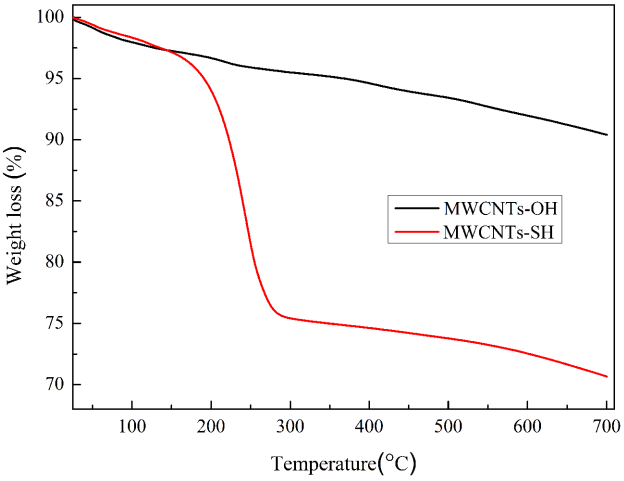

Fig. 2. TGA curves of MWCNTs–OH and MWCNTs–SH with the atmosphere of argon.

Table 1
Elemental composition (%) of functionalized MWCNTs

Materials	MWCNTs–OH	MWCNTs–SH
N, %	0.138	0.226
C, %	90.35	74.95
H, %	0.343	0.083
S, %	0.094	22.81

According to the experiments, the S–H or C–S bond should appear in MWCNTs–SH, but hardly detectable in the FT-IR spectra. Therefore, to confirm the presence of –SH groups on the MWCNTs–SH surface, the XPS was used. The XPS survey spectra for the MWCNTs–OH and MWCNTs–SH are shown in Fig. 3. The main peak (C1s) was observed at the binding energy (BE) of 284.82 eV. The peak component at the BE of 532.85 eV is assigned to O1s of the hydroxy groups on the surface of MWCNTs [28]. The S2p peak appeared at the BE of 164.36 eV (as shown in Fig. 3(b)), which is due to the $–CH_2–SH$ bond on MWCNTs [29]. The XPS results of MWCNTs–SH verify that the thiol groups are successfully anchored onto the MWCNTs.

Fig. 4 displays the representative SEM images of the MWCNTs, MWCNTs–OH, and MWCNTs–SH, which shows that these materials are usually curves and have cylindrical shapes. As seen from Fig. 4(a), the raw MWCNTs had diameter in the range of 20–40 nm and length over 5 μm. And no detectable changes in the surface morphology can be observed among all the samples. The nanotubes did not appear to be damaged or shorted during the functionalization, washing and drying procedures. However, there are more identifiable gold patches (bright patches) on the MWCNTs–OH and MWCNTs–SH than on the r-MWCNTs, which suggested that the materials become more active at the ends and sidewalls due to functionalization [30]. There are created defect sites and covalently attached functional groups during the functionalization, which can cause the electric conductivity of the nanotube bundles to be reduced. This causes partial blurring of the images of the functionalized MWNTs, which results in reduction of the contrast and resolution [31].

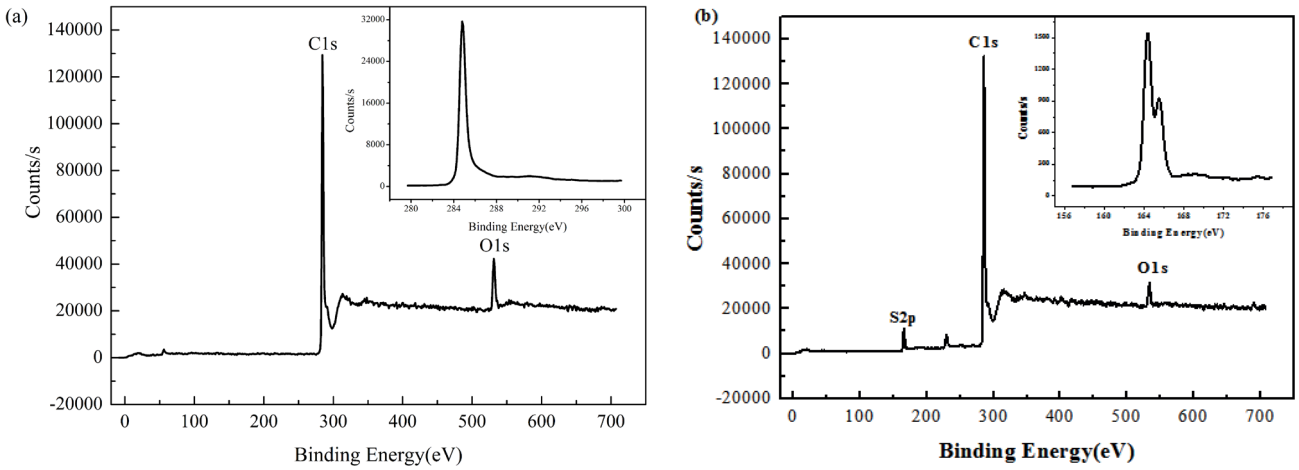

Fig. 3. XPS spectra of wide scan of the (a) MWCNTs–OH and (b) MWCNTs–SH.

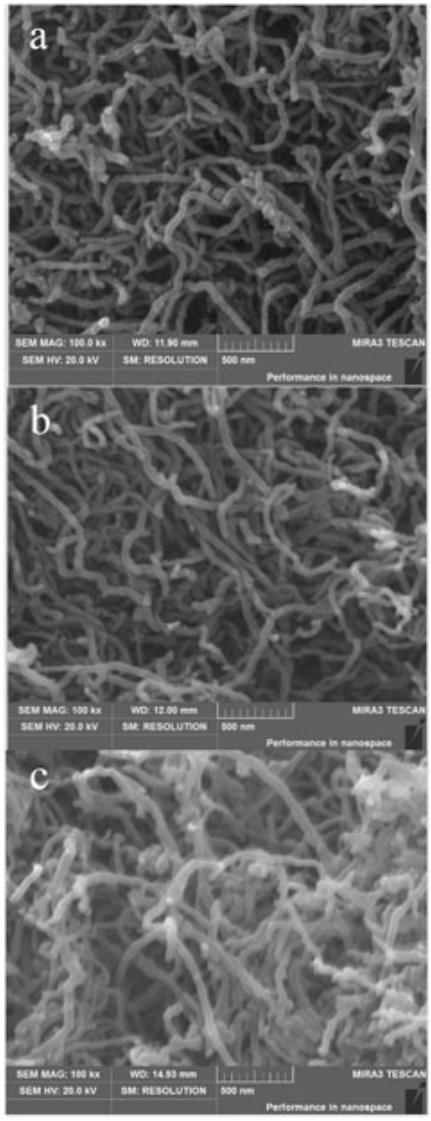

Fig. 4. SEM images of (a) r-MWCNTs MWCNTs, (b) MWCNTs–OH and (C) MWCNTs–SH.

3.2. Effect of solution pH

The pH of the solution plays an important role on the adsorption of heavy ion metals. In order to study the effect of pH on the adsorption of Cd(II) and Pb(II) on the MWCNTs–SH, experiments were carried out with various pH. The pH of solution was adjusted by using diluted HNO_3 and NaOH solution. Fig. 5 shows that both the adsorption capacity of Cd(II) and Pb(II) present increasing trend with the rise of pH value. Furthermore, it can be observed that the adsorption capacity of Pb(II) was higher than that of Cd(II). This could be explained by the Pearson's theory that soft ligands like thiol groups are more likely to attract soft metals. Generally speaking, Pb(II) is softer than Cd(II). The increase of adsorption for Cd(II) and Pb(II) with the increasing solution pH may be mainly attributed to the following two reasons. Firstly, the competitive interaction between metal ions and proton with thiol groups decreased in higher pH, which may lead to the increase of the adsorption capacity. Secondly, the heavy metal ions have the tendency to form $M(OH)^+$(aq) at higher pH values, which have smaller hydrated sizes than M^{2+}(aq) due to their lower charges and thus greater accessibility to the porous structure of adsorbents [32], resulting in the increase of adsorption capacity. But metal hydroxides would precipitate with further increasing pH. Therefore, the pH values of the solution were fixed at 6.0 and 5.0 for the adsorption of Cd(II) and Pb(II).

3.3. Adsorption isotherms

Numerous adsorption isotherms are employed to describe the interaction between adsorbents and adsorbates. In this study, two classical adsorption isotherm models, namely Langmuir and Freundlich equations, were used to describe the adsorption of Cd(II) and Pb(II) onto the MWCNTs–SH surfaces.

The Langmuir isotherm is based on a monolayer adsorption of metal ions on the surface of the adsorbents and can be expressed by the following equation [33]:

$$\frac{C_e}{q_e} = \frac{C_e}{q_m} + \frac{1}{q_m k_d} \quad (2)$$

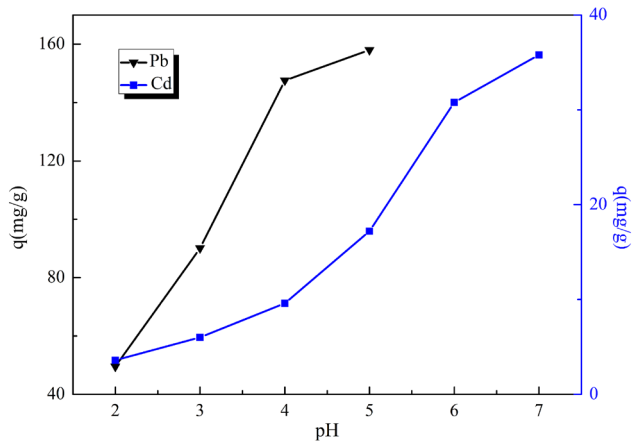

Fig. 5. Effect of pH on the adsorption of Cd(II) and Pb(II) by MWCNTs–SH at 25°C, the volume of Cd(II) and Pb(II) were 20 mL and 30 mL, respectively.

where C_e is the equilibrium concentration of metal ions in solution (mg/g), q_e the adsorption capacity of adsorbent at equilibrium(mg/g). The q_m is the maximum adsorption capacity (mg/g) and k_d is the Langmuir constant which is related to the affinity bonding energy of adsorption. The values of k_d and q_m are obtained from the slope and the intercept of the C_e/q_e vs. C_e.

The Freundlich isotherm is considered to be an empirical equation for describing both multi-layer adsorption and adsorption on heterogeneous surfaces. This isotherm equation can be represented as follows [34]:

$$\ln q_e = \ln k_f + \frac{1}{n}\ln C_e \tag{3}$$

where k_f and 1/n are physical constants of Freundlich isotherm, k_f is the indicator of adsorption capacity and $1/n$ is the measurement of adsorption effectiveness. The values of k_f and 1/n can be obtained from the intercept and slope of the linear Freundlich equation.

Adsorption isotherms contain certain parameters related to the surface properties of the adsorbents, and made it possible to evaluate the adsorption capacity of the adsorbent for heavy metal ions. Fig. 6 shows the adsorption isotherms of Cd(II) and Pb(II) onto MWCNTs–SH surfaces at pH 6.0 and 5.0, respectively. The isotherm parameters are obtained through fitting the adsorption equilibrium data to the Langmuir and Freundlich isotherm models, and are listed in Table 2. It can be noticed that the correlation coefficients values (R^2) for the Langmuir isotherm model are higher than the Freundlich isotherm models, thus indicating that the Langmuir model better describes adsorption onto MWCNTs–SH. Therefore, the adsorption of MWCNTs–SH of Cd(II) and Pb(II) ions can be mainly considered as monolayer adsorption. As seen from Table 2, both the q_{max} and k_d values increase with the increasing temperature, while the R^2 remain similar. These values suggested possibly use of MWCNTs–SH for adsorption Cd(II) and Pb(II) ions from polluted water at higher temperature. Moreover, the maximum adsorption capacity of Cd(II) and Pb(II) are 157.73 and 187.27 mg/g at 25°C, respectively. A comparison of the present MWCNTs–SH with those different types of CNTs in recent references is shown in Table 3.

3.4. Adsorption kinetics

In order to show the most suitable adsorption kinetic model of Cd(II) and Pb(II) onto the surface of MWCNTs–SH, the pseudo-first-order, pseudo-second-order equation were used to fit the experimental data in this study.

The pseudo-first-order rate equation is based on the assumption that the chemisorption rate limiting step given by [35]:

$$\ln(q_e - q_t) = \ln q_e - \frac{k_1}{2.303}t \tag{4}$$

where q_t is the adsorption capacity at any time (mg/g), and q_e is the amount of metal ions at equilibrium (mg/g). k_1 is the rate constant of pseudo-first-order adsorption (1/min).

The pseudo-second-order rate is based on the adsorption capacity of the solid phase and is expressed by the following equation [34]:

$$\frac{t}{q_t} = \frac{1}{k_2 q_e^2} + \frac{1}{q_e}t \tag{5}$$

where k_2 is the rate constant of pseudo-second-order adsorption (g/mg·min).

The typical kinetic experimental curves for adsorption of Cd(II) and Pb(II) ions on the MWCNTs–SH were shown in Fig. 7(a). The ion adsorption increased sharply during the first 20 min and then slowed down gradually to reach equilibrium. It is possible that, in the early stage, the surface coverage of the MWCNTs–SH is relatively low, and the heavy metal ions are beneficial to occupy the active surface site rapidly at random. The rate of adsorption of metal ions in the later stage becomes slower because the active surface sites of the MWCNTs–SH are occupied by heavy metal ions. Ultimately, the surface of adsorbent becomes saturated, reaching the saturation adsorption. It can be seen from Fig. 7(a) that the adsorption capacity of Cd(II) and Pb(II) were 37.88 and 198.78 mg/g, respectively. So the contact time for adsorption studies was maintained at 60 min throughout all the experiments.

The parameters and the correlation coefficients values (R^2) for the two kinetic equations were shown in Table 4. Taking the adsorption of Cd(II) on the MWCNTs–SH, for example, the R^2 value of the pseudo-second-order equation (R^2 = 0.999) was higher than the results obtained from the pseudo-first-order equation (R^2 = 0.977), indicating that the adsorption behavior better fit to pseudo-second-order model. Similar performance can be observed in the adsorption of Pb(II). Therefore, the adsorption behavior of Cd(II) and Pb(II) onto MWCNTs–SH fitted well with the pseudo-second-order equation. And the fitting lines of the adsorption of Pb(II) and Cd(II) by pseudo-second-order and pseudo-first-order equation were shown in Fig. 7(b) and Fig. 7(c).

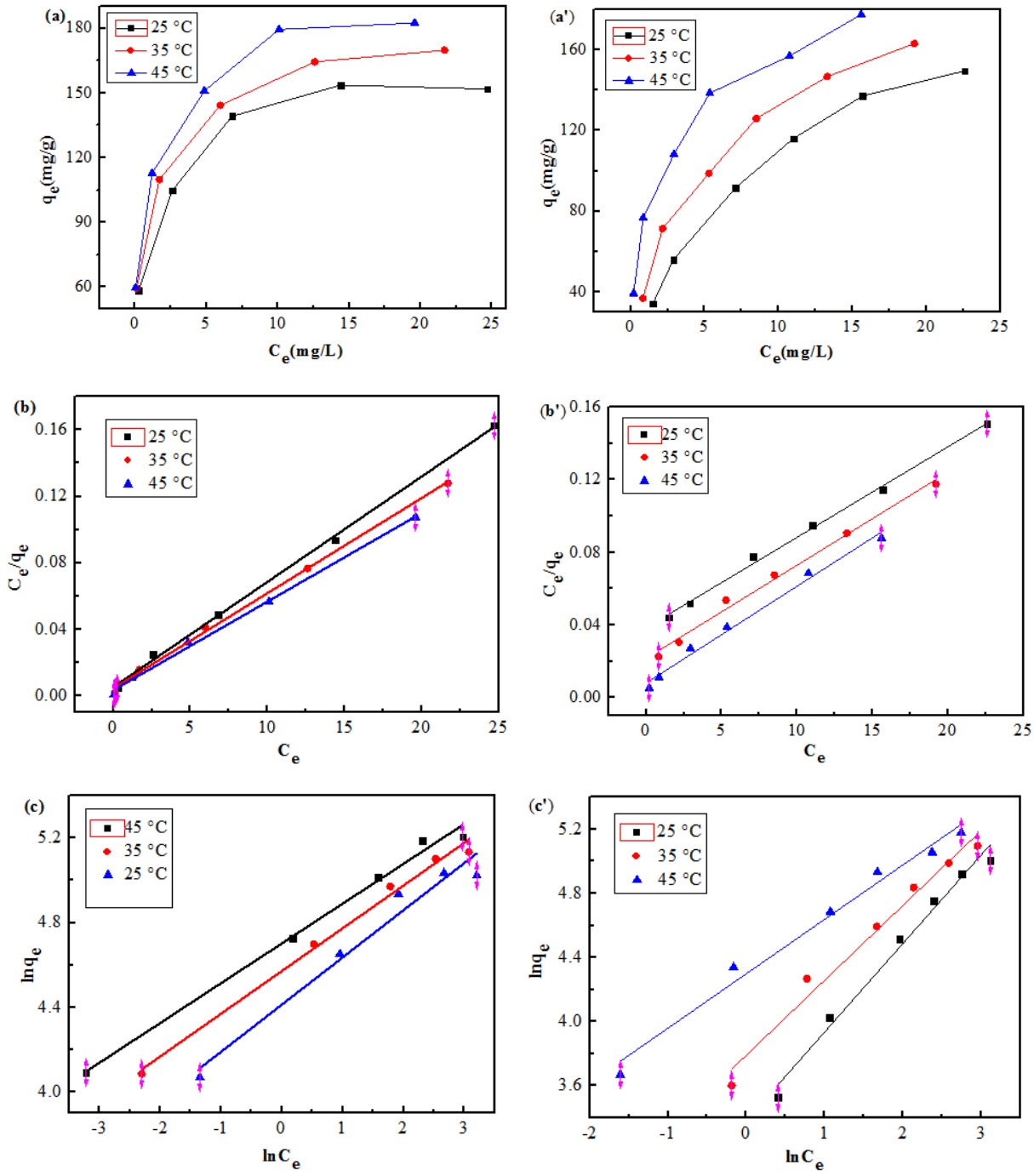

Fig. 6. (a) Adsorption isotherms of Pb(II) by MWCNTs–SH, the initial concentrations of Pb(II) were changed from 10 to 60 mg/L, the volume was 30 mL; (a') adsorption isotherms of Cd(II) by MWCNTs–SH, the initial concentrations of Cd(II) were changed from 10 to 50 mg/L, the volume was 30 mL; (b) Langmuir isotherms for the adsorption of Pb(II); (b') Langmuir isotherms for the adsorption of Cd(II); (c) Freundlich isotherms for the adsorption of Pb(II); (c') Langmuir isotherms for the adsorption of Cd(II).

3.5. Adsorption thermodynamics

The standard Gibbs free energy changes (ΔG^{θ}), standard enthalpy changes (ΔH^{θ}), and standard entropy changes (ΔS^{θ}) of the adsorption process were calculated using the following thermodynamic equations [36]:

$$\ln k_a = \frac{\Delta G^{\theta}}{R} - \frac{\Delta H^{\theta}}{RT} \tag{6}$$

$$\Delta G^{\theta} = \Delta H^{\theta} - T\Delta S^{\theta} \tag{7}$$

Table 2
Fitting results with Langmuir and Freundlich isotherm for Pb(II) and Cd(II) by MWCNTs–SH

Metal ions	Parameter value	Langmuir isotherm			Freundlich isotherm		
		q_m(mg/g)	k_d	R^2	n	k_f	R^2
Pb(II)	298.15 K	187.27	1.243	0.998	4.478	82.426	0.953
	308.15 K	194.55	1.306	0.997	4.948	96.631	0.989
	318.15 K	200.40	1.643	0.997	5.312	110.112	0.990
Cd(II)	298.15 K	157.73	0.130	0.996	1.812	29.438	0.982
	308.15 K	173.61	0.239	0.990	2.141	44.259	0.974
	318.15 K	187.23	0.673	0.987	2.949	73.577	0.979

Table 3
A comparison for the maximum adsorption capacities of functionalized MWCNTs with those of some other MWCNTs reported in literatures for the adsorption of Cd(II) and Pb(II)

Adsorbent	Metal ions	q_m (mg/g)	T (°C)	pH	Ref.
Ethylenediamine MWCNTs	Cd(II)	25.70	45	8.0	[12]
Triethylenediamine MWCNTs	Cd(II)	31.45	45	8.0	[38]
	Pb(II)	58.26		6.2	
Oxidized carbon nanotubes sheets	Cd(II)	75.84	–	–	[39]
MWCNTs/PAAM	Pb(II)	28.12	20	5.0	[40]
MPTS–CNTs/Fe_3O_4	Pb(II)	65.40	25	6.5	[23]
MWCNTs–SH	Cd(II)	157.73	25	6.0	This
	Pb(II)	187.27		5.0	study

where T is the absolute temperature(K) and R the universal gas constant(8.314 J/mol·K). The values of ΔS^θ and ΔH^θ were calculated from the intercept and slope of the plots of lnk_d vs. 1/T plot. K_d is the equilibrium distribution coefficient for the adsorption process which was calculated from the initial and the equilibrium concentrations (C_o and C_e) of the metal ions:

$$k_d = \frac{C_o - C_e}{C_e} \times \frac{V}{m} \tag{8}$$

where V is the volume of the solution (L), and m is the dosage of the adsorbent (g).

The effect of temperature on the adsorption of Cd(II) and Pb(II) ions onto MWCNTs–SH was illustrated in Fig. 6(a') and Fig. 6(a), respectively. The values of thermodynamic parameters including ΔH^θ, ΔS^θ and ΔG^θ calculated from Eqs. (6)–(8) are summarized in Table 5, which gave useful information about the adsorption mechanism of Cd(II) and Pb(II) ions onto MWCNTs–SH.

As seen from Table 5, the initial concentrations of Cd(II) and Pb(II) solution are ranged from 10 to 50 and 10 to 60 mg/L, respectively. The positive values of ΔH^θ indicated that the adsorption of MWCNTs–SH for Cd(II) and Pb(II) were endothermic processes. Furthermore, the positive values of ΔS^θ demonstrated a tendency to higher disorder at the solid/solution interface during the adsorption. And the increase of the randomness of the system may be related to the liberation of water of hydration and the ion

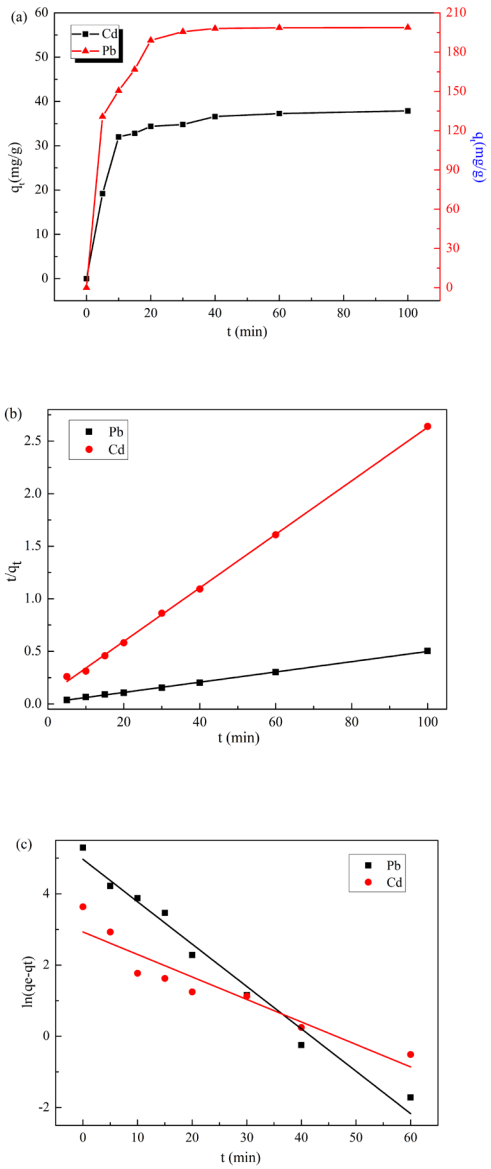

Fig. 7. (a) Effect of time on the adsorption of Cd(II) and Pb(II) by MWCNTs–SH at 25°C, the volume of Cd(II) and Pb(II) were 20 mL and 30 mL, respectively; (b) pseudo-second-order kinetic for the adsorption of Cd(II) and Pb(II); (c) pseudo-first-order kinetic for the adsorption of Cd(II) and Pb(II).

Table 4
Kinetic parameters for the Pb(II) and Cd(II) adsorption by MWCNTs–SH

Equations	Parameters	Metal ions	
		Pb(II)	Cd(II)
Pseudo-first-order kinetic	q_e, exp (mg/g)	198.87	37.88
	q_e, cal (mg/g)	143.55	18.72
	k_1 (min^{-1})	0.145	0.274
	R^2	0.977	0.876
Pseudo-second-order kinetic	q_e, cal (mg/g)	205.34	39.28
	k_2 ($min \times 10^{-3}$)	1.925	7.545
	R^2	0.999	0.999

Table 5
Thermodynamic parameters for the adsorption of Pb(II) and Cd(II) by MWCNTs–SH

Metal ions	C_0 (mg/L)	ΔH^θ (kJ/mol)	ΔS^θ (J/mol/K)	$-\Delta G^\theta$ (kJ/mol) at temperature		
				298.15 K	308.15 K	318.15 K
Pb(II)	10	74.964	296.847	13.559	16.509	19.496
	20	33.597	143.685	9.243	10.680	12.116
	30	16.509	80.435	7.473	8.277	9.081
	40	20.107	87.067	5.852	6.723	7.593
	50	16.457	70.455	4.549	5.254	5.958
	Mean	32.327	135.698	8.135	9.489	10.849
Cd(II)	10	84.825	309.739	7.524	10.621	13.718
	20	60.643	227.648	7.230	9.507	11.783
	30	41.434	159.998	6.269	7.869	9.469
	40	35.420	138.254	5.800	7.183	8.566
	50	20.289	86.096	5.381	6.241	7.102
	60	21.425	87.613	4.697	5.573	6.449
	Mean	43.339	168.225	6.150	7.832	9.515

exchange [37]. Finally, the negative value of ΔG^θ indicates the spontaneity and feasibility of the adsorption of Cd(II) and Pb(II) on the adsorbent.

4. Conclusion

In this study, MWCNTs–SH was synthesized by a highly efficient, inexpensive, and simple method, and used as adsorbents for removing Pb(II) and Cd(II) from aqueous solutions. The characteristic results of EA, SEM, XPS, and TGA showed that the thiol groups were introduced onto the MWCNTs successfully. Adsorption kinetic and isotherm processes for metal ions were found to correlate with pseudo-second-order model and Langmuir isotherm equation. Furthermore, free energy changes were –8.135 and –6.150 KJ/mol for Pb(II), Cd(II) at 25°C, which revealed that the adsorption processes were spontaneous. Therefore, the composite of MWCNTs–SH is a very suitable material for heavy metal ions pollution cleanup because of the strong affinity of thiol groups. Through the work described in this article, the methods of introducing thiol groups onto MWCNTs will be probably extended, the synthetic material is also relevant and important for the application of CNTs in the natural environment cleanup.

Acknowledgement

This work was supported by the National Natural Science Foundation of China (No. 21571191 and No. 21471163).

References

[1] F.N. Acar, Z. Eren, Removal of Cu(II) ions by activated poplar sawdust (Samsun Clone) from aqueous solutions, J. Hazard. Mater., 137 (2006) 909–914.
[2] A.M. Choi, J. Alam, Heme oxygenase-1: function, regulation, and implication of a novel stress-inducible protein in oxidant-induced lung injury, Am. J. Respir. Cell. Mol. Biol., 15 (1996) 9–19.
[3] L.R. Bravo-Sánchez, B.S.V. de la Riva, J.M. Costa-Fernández, R. Pereiro, A. Sanz-Medel, Determination of lead and mercury in sea water by preconcentration in a flow injection system followed by atomic absorption spectrometry detection, Talanta, 55 (2001) 1071–1078.
[4] M.M. Saeed, M. Ahmed, Retention, kinetics and thermodynamics profile of cadmium adsorption from iodide medium onto polyurethane foam and its separation from zinc bulk, Anal. Chim. Acta., 525 (2004) 289–297.
[5] J.L. Gong, B. Wang, G.M. Zeng, C.P. Yang, C.G. Niu, Q.Y. Niu, Y. Liang, Removal of cationic dyes from aqueous solution using magnetic multi-wall carbon nanotube nanocomposite as adsorbent, J. Hazard. Mater., 164 (2009) 1517–1522.

[6] M.M. Matlock, B.S. Howerton, D.A. Atwood, Chemical precipitation of heavy metals from acid mine drainage, Water Res., 36 (2002) 4757–4764.
[7] C.H. Liu, J.S. Wu, H.C. Chiu, S.Y. Suen, K.H. Chu, Removal of anionic reactive dyes from water using anion exchange membranes as adsorbers, Water Res., 41 (2007) 1491–1500.
[8] G. Capar, U. Yetis, L. Yilmaz, Membrane based strategies for the pre-treatment of acid dye bath wastewaters, J. Hazard. Mater., 135 (2006) 423–430.
[9] R. De Lisi, G. Lazzara, S. Milioto, N. Muratore, Adsorption of a dye on clay and sand. Use of cyclodextrins as solubility-enhancement agents, Chemosphere., 69 (2007) 1703–1712.
[10] K. Kadirvelu, K. Thamaraiselvi, C. Namasivayam, Removal of heavy metals from industrial wastewaters by adsorption onto activated carbon prepared from an agricultural solid waste, Bioresour. Technol., 76 (2001) 63–65.
[11] D. Sud, G. Mahajan, M.P. Kaur, Agricultural waste material as potential adsorbent for sequestering heavy metal ions from aqueous solutions – a review, Bioresour. Technol., 99 (2008) 6017–6027.
[12] T. Panczyk, M. Drach, P. Szabelski, A. Jagusiak, Magnetic anisotropy effects on the behavior of a carbon nanotube functionalized by magnetic nanoparticles under external magnetic fields, J. Phys. Chem. C., 116 (2012) 26091–26101.
[13] R.H. Baughman, A.A. Zakhidov, W.A. de Heer, Carbon nanotubes – the route toward applications, Science., 297 (2002) 787–792.
[14] O. Moradi, K. Zare, M. Monajjemi, M. Yari, H. Aghaie, The studies of equilibrium and thermodynamic adsorption of Pb(II), Cd(II) and Cu(II) ions from aqueous solution onto SWCNTs and SWCNT-COOH surfaces, Fuller. Nanotub. Car. N., 18 (2010) 285–302.
[15] G.-P. Rao, C. Lu, F. Su, Sorption of divalent metal ions from aqueous solution by carbon nanotubes: a review, Sep. Purif. Technol., 58 (2007) 224–231.
[16] Z. Gao, T.J. Bandosz, Z. Zhao, M. Han, C. Liang, J. Qiu, Investigation of the role of surface chemistry and accessibility of cadmium adsorption sites on open-surface carbonaceous materials, Langmuir., 24 (2008) 11701–11710.
[17] G.D. Vuković, A.D. Marinković, S.D. Škapin, M.D. Ristić, R. Aleksić, A.A. Perić-Grujić, P.S. Uskoković, Removal of lead from water by amino modified multi-walled carbon nanotubes, Chem. Eng. J., 173 (2011) 855–865.
[18] G.D. Vuković, A.D. Marinković, M. Čolić, M.D. Ristić, R. Aleksić, A.A. Perić-Grujić, P.S. Uskoković, Removal of cadmium from aqueous solutions by oxidized and ethylenediamine-functionalized multi-walled carbon nanotubes, Chem. Eng. J., 157 (2010) 238–248.
[19] J.P. Hu, J.H. Shi, S.P. Li, Y.J. Qin, Z.X. Guo, Y.L. Song, D.B. Zhu, Efficient method to functionalize carbon nanotubes with thiol groups and fabricate gold nanocomposites, Chem. Phys. Lett., 401 (2005) 352–356.
[20] Z.F. Liu, Z.Y. Shen, T. Zhu, S.F. Hou, L.Z. Ying, Z.J. Shi, Z.N. Gu, Organizing single-walled carbon nanotubes on gold using a wet chemical self-assembling technique, Langmuir., 16 (2000) 3569–3573.
[21] M. Hadavifar, N. Bahramifar, H. Younesi, Q. Li, Adsorption of mercury ions from synthetic and real wastewater aqueous solution by functionalized multi-walled carbon nanotube with both amino and thiolated groups, Chem. Eng. J., 237 (2014) 217–228.
[22] N.M. Bandaru, N. Reta, H. Dalal, A.V. Ellis, J. Shapter, N.H. Voelcker, Enhanced adsorption of mercury ions on thiol derivatized single wall carbon nanotubes, J. Hazard. Mater., 261 (2013) 534–541.
[23] C. Zhang, J. Sui, J. Li, Y. Tang, W. Cai, Efficient removal of heavy metal ions by thiol-functionalized superparamagnetic carbon nanotubes, Chem. Eng. J., 210 (2012) 45–52.
[24] Q. Li, J.G. Yu, F. Zhou, X.Y. Jiang, Synthesis and characterization of dithiocarbamate carbon nanotubes for the removal of heavy metal ions from aqueous solutions, Colloid. Surface A., 482 (2015) 306–314.
[25] M.H. Hsu, H. Chuang, F.Y. Cheng, Y.P. Huang, C.C. Han, K.C. Pao, D.S. Wu, Simple and highly efficient direct thiolation of the surface of carbon nanotubes, RSC. Adv., 4 (2014) 14777–14780.
[26] B. Šljukic, C.E. Banks, R.G. Compton, Iron oxide particles are the active sites for hydrogen peroxide sensing at multiwalled carbon nanotube modified electrodes, Nano. Lett., 6 (2006) 1556–1558.
[27] J. Xu, P. Yao, X. Li, F. He, Synthesis and characterization of water-soluble and conducting sulfonated polyaniline/para-phenylenediamine-functionalized multi-walled carbon nanotubes nano-composite, Mater. Sci. Eng. B-Adv., 151 (2008) 210–219.
[28] J. Hu, J. Shi, S. Li, Y. Qin, Z.X. Guo, Y. Song, D. Zhu, Efficient method to functionalize carbon nanotubes with thiol groups and fabricate gold nanocomposites, Chem. Phys. Lett., 401 (2005) 325–356.
[29] Y.Z. You, C.Y. Hong, C.Y. Pan, Functionalization of carbon nanotubes with well-defined functional polymers via thiol-coupling reaction, Macromol. Rapid. Comm., 27 (2006) 2001–2006.
[30] Y.S. Kim, J.H. Cho, S.G. Ansari, H.I. Kim, M.A. Dar, H.K. Seo, H.S. Shin, Immobilization of avidin on the functionalized carbon nanotubes, Synth. Met., 156 (2006) 938–943.
[31] Y. Wang, Z. Iqbal, S.V. Malhotra, Functionalization of carbon nanotubes with amines and enzymes, Chem. Phys. Lett., 402 (2005) 96–101.
[32] B. Xiao, K.M. Thomas, Adsorption of aqueous metal ions on oxygen and nitrogen fictionalized nanoporous activated carbons, Langmuir., 21 (2005) 3892–3902.
[33] Y. Xie, D. Qian, D. Wu, X. Ma, Magnetic halloysite nanotubes/iron oxide composites for the adsorption of dyes, Chem. Eng. J., 168 (2011) 959–963.
[34] F. He, J. Fan, D. Ma, L. Zhang, C. Leung, H.L. Chan, The attachment of Fe_3O_4 nanoparticles to graphene oxide by covalent bonding, Carbon, 48 (2010) 3139–3144.
[35] S. Azizian, Kinetic models of sorption: a theoretical analysis, J. Colloid Interf. Sci., 276 (2004) 47–52.
[36] A.A. Farghali, M. Bahgat, W.M. ElRouby, M.H. Khedr, Decoration of multi-walled carbon nanotubes (MWCNTs) with different ferrite nanoparticles and its use as an adsorbent, J. Nanostruct. Chem., 3 (2013) 1–12.
[37] G.P. Rao, C. Lu, F. Su, Sorption of divalent metal ions from aqueous solution by carbon nanotubes: a review, Sep. Purif. Technol., 58 (2007) 224–231.
[38] G.D. Vukovic, A.D. Marinkovic, S.D. Skapin, Removal of lead from water by amino modified multi-walled carbon nanotubes, Chem. Eng. J., 173 (2011) 855–865.
[39] E. Nieboer, D.H.S. Richardson, The replacement of the nondescript term 'heavy metals' by a biologically and chemically significant classification of metal ions, Environ. Pollu. Series B, Chem. and Phys., 1 (1980) 3–26.
[40] S. Yang, J. Hu, C. Chen, Mutual effects of Pb (II) and humic acid adsorption on multiwalled carbon nanotubes/polyacrylamide composites from aqueous solutions, Environ. Sci. & Technol., 45 (2011) 3621–3627.